Journal of Economic Behavior and Organization 248 (2026) 107609

Contents lists available at ScienceDirect

Journal of Economic Behavior and Organization

journal homepage: www.elsevier.com/locate/jebo

Cyclical behavior in large location games☆

Gary Charness [a,1], Daniel Friedman [b,c,*], Weinan Gong [c], Lones Smith [d,2]

[a] Formerly with University of California, Santa Barbara, USA
[b] University of Essex, United Kingdom
[c] University of California Santa Cruz, United States of America
[d] University of Wisconsin, Madison, United States of America

ARTICLE INFO

JEL classification:
C63
C73
C92
D90.

Keywords:
Population game
Laboratory experiment
Agent based simulations
Cycles

ABSTRACT

Location games capture important economic phenomena ranging from preemption to choice of bank leverage. We explore a parametric family of location games with many players, each facing a conflict between maximizing a fundamental payoff component and a relative (or quantile dependent) component. Using simulations and human subject experiments we show that, behaviorally, the stationary Nash equilibria in such games are terrible predictions of behavior and payoffs when players can freely adjust their locations. Instead, large cycles consistently emerge, in which behavior slowly grows bolder over time. This corresponds to progressively earlier timing in pre-emption games or to increasingly later timing in wars of attrition. When locations are maximally bold, namely at the end of the domain of Nash play, behavior quickly reverts to the peak fundamental and a new cycle begins.

1. Introduction

"And yet it moves".

[Galileo Galilei]

Location games capture economic settings with an intensity choice. For instance, how much of one's financial portfolio should be in stocks versus bonds? How much leverage should one take on an investment? How much time should one allocate to leisure versus work? How large a house should one purchase, or how far should it be from work? In many such settings, your payoff depends not merely on your own choice, but where it lands in the distribution. A portfolio heavily weighted towards stocks is not so risky if more people are doing so, lending more stability to stock prices. A smaller downpayment on a loan leads to a lower interest rate if the bank finds that more borrowers are also opting for less money down. A house farther from work is less of a hassle if more coworkers also choose a distant location, increasing the likelihood that work-from-home will be offered.

We build on the work of Anderson et al. (2017) (hereafter, ASP), who analyze a broad class of location games with a continuum of players. ASP interpret location as stopping time, and their class of games subsumes wars of attrition and pre-emption games as

☆ This article is part of a Special issue entitled: 'A Tribute to the Work of Gary Charness' published in Journal of Economic Behavior and Organization.

* Corresponding author at: University of California Santa Cruz, United States of America.
E-mail addresses: dan@ucsc.edu (D. Friedman), wgong4@ucsc.edu (W. Gong), lones.smith@gmail.com (L. Smith).

[1] Deceased.

[2] We are grateful to Peter Bossaerts, Guillaume Frechette, Catherine Eckel, Charlie Holt, and Matt Jackson for helpful comments, and to audiences at a LearningEvolutionGames webinar (March 2023), at Cambridge (October 2023), and at the Tucson GaryFest (January 2025). The final version owes much to the thoughtful comments of the GEB review team. We are also indebted to Zev Cooper for building software prototypes. This project is dedicated to the memory of Gary Charness (1950–2024), who initially proposed it and guided its development until his final days.

https://doi.org/10.1016/j.jebo.2026.107609
Received 1 April 2025; Received in revised form 12 March 2026; Accepted 11 May 2026
Available online 20 May 2026

special cases.[3] Payoffs in ASP reflect two factors: the stopping time, which fixes the fundamental payoff, and stopping quantile. Thus all strategic interaction is filtered through a player's position in the action distribution. As the quantile preference shifts from a desire to stop earlier to later in the distribution, the game suggestively transitions from *greed* (for higher rank payoffs in a war of attrition) to *fear* (of missing out in a pre-emption game). ASP characterize "safe" Nash equilibria that are robust to slight location mistakes.[4] Such equilibria entail play at every point along an interval from the *harvest time* — the point that maximizes the fundamental payoff component — either to a specific earlier or to a later location, where lower fundamental payoffs are compensated by a preferred quantile.

The present paper explores a rich parametric subclass of ASP in which payoffs are the product of a quadratic location factor and a quadratic quantile factor. In a laboratory experiment we find that Nash equilibrium is highly misleading prediction of human behavior. We allow a dozen or so players to freely adjust their location in real time, and observe systematically non-stationary behavior. The asymptotic and the time-average observed behavior and realized payoffs, all are far from safe Nash equilibrium. Instead, the robust laboratory outcome is perpetual large cycles. Average behavior in such cycles shows no evidence of the rushes (jumps in the cdf) that feature prominently in ASP. Observed behavior grows bolder over time: progressively earlier in pre-emption games, and increasingly later in wars of attrition. Eventually, players jump back to the harvest time, and the cycle resumes. Moreover, average observed payoffs consistently exceed the Nash payoffs.

Is there some plausible adjustment dynamic that approaches the Nash equilibrium? We run simulations of boundedly rational agents ("bots"), programmed to myopically optimize when their number is called. Each bot is initially assigned a location. The simulation consists of many time steps, and in each step each bot earns the payoff determined by her location and quantile in the current distribution of bot locations. Each time step, a specified fraction of the bots (e.g., 20%) are allowed to freely adjust their location, and they choose the location with highest payoff, to which we add a little noise. (This is a stylized version of our laboratory setup, which allows completely free form optimization of location, constrained only by technology: the real time latency between adjustment opportunities is short, a second or half second, so that typically only a fraction of other human traders adjust their actions at the same opportunity.) To check robustness, we vary the number of bots, the fraction that move each time step, the noise amplitude, etc.

In all simulations, cycles emerge. Their domain, frequency, and average payoffs depend on the payoff (quantile and location) parameters. The bots' chosen locations lie in the support interval of the Nash equilibrium, but their time-averaged distribution is much more uniform and overall payoffs are higher than in the Nash equilibrium.

We use the simulation outcomes and the Nash equilibrium as alternative theoretical predictions of behavior observed in the human player experiment. The main finding is that human subjects and bots exhibit the same major systematic major deviations from Nash play: large cycles emerge, with average play far from Nash, and average payoffs above Nash. By and large, we confirm the comparative statics obtained from the simulations. For example, as we vary the payoff function parameters, (1) humans reliably choose locations within the parameter-specific interval that supports simulated cycles (and Nash equilibrium); (2) the observed distribution of human-chosen locations is closer to that of the bots (approximately uniform) than to that of Nash equilibrium, which features jumps for some parameters; (3) the frequency of observed cycles in the experiment is positively correlated with the simulated cycle frequency; and (4) humans as well as bots tend to make fewer and larger location changes moving towards the harvest time than changes moving away from it.

Literature. Location games capture important economic phenomena. A venerable literature, dating back to Veblen (1899), considers the consequences when each consumer chooses the degree of conspicuous consumption. Standard models in urban economics feature workers who choose the commute distance from an urban center.

An influential location game close in flavor to ours is the instructive analysis of the Keynesian Beauty Contest in Morris and Shin (2002), where everyone desires to be closest to a weighted average of their personal and their estimated fundamental best. This resembles our dual payoff objective of a fundamental and a quantile consideration.

Cyclical or nonstationary behavior has been observed in markets with a location structure. As noted in Geanakoplos (2009), the leverage cycle, with gradually falling loan down payments or collateral requirements, is a financial regularity in the lending market — and arguably played a major role in the 2008–9 Financial Crisis. This cycle reflects a game with our strategic flavor, and the cycle is as we predict: behavior grows bolder and riskier over time, until the moment arrives when everyone shifts back to playing it safe.

Roth and Xing (1994) notably deduced nonstationary outcomes of entry-level professional labor markets — such as Federal court clerkships in law firms. This corresponds to our fear equilibrium, with a trend towards earlier and earlier matching until that becomes untenable.

A large literature explores standard finite action games with mixed equilibria, like rock-paper scissors, and sometimes finds cyclical behavior, e.g., Cason et al. (2014). Our results do not hinge on whether or not individual players are able to employ an equilibrium mixed strategy. Indeed, ASP show that there are arbitrarily close games, in which every player has a unique pure strategy best reply in equilibrium. Rather, our cycles emerge in location games with conflicting fundamental and quantile location incentives.

[3] Intuitively, even though these are timing games with pre-commitment, they have similar comparative statics as the truly dynamic timing games solved with subgame perfect or sequential equilibrium.

[4] The "safe" refinement excludes Nash equilibria in which everyone chooses precisely the same location near the harvest time, because then the quantile jumps to 0 or 1 with the slightest of mistakes.

Table 1
Terminology and notation.

Term	Notation	Comment
Fund'lFactor	$u(x)$	Payoff factor depending on location x
HarvestTime	$\hat{x}$	Location at which $u(x)$ achieves its maximum
QuantileFactor	$v(q)$	Payoff factor depending on relative location $q = Q(x)$.
Gradual play	$Q'(x) > 0$	Interval of points where cdf Q has a positive density
Rush	Q jumps	Positive mass of players choose identical location x
Landscape	$u(x)v(Q(x))$	Payoff as a function of location x given current cdf Q
NashSupport	Supp$[Q^{NE}]$	Includes all rush and gradual play points in a NE cdf.
Fear (FOMO)	$u'(x) > 0 > v'(q)$	Local preemption: $x \uparrow \Longrightarrow u \uparrow$ but $v \downarrow$ in Supp$[Q^{NE}]$
Greed	$u'(x) < 0 < v'(q)$	Local war of attrition: $x \uparrow \Longrightarrow u \downarrow$ but $v \uparrow$

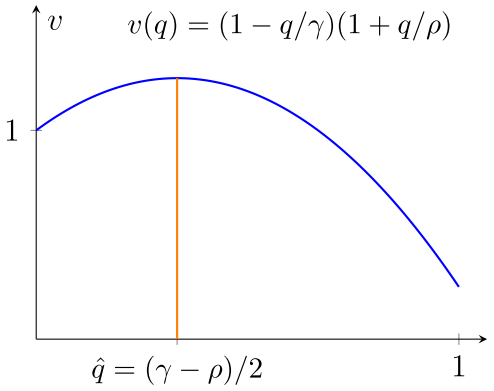

Fig. 1. Quantile Factor Plot.

One of the more widely studied applications of location games is to pricing, and cyclical pricing behavior has been discussed at least since Edgeworth (1925). Cason et al. (2005, 2021) find price cycles in a price search experiment based on Burdett and Judd (1983). Noel (2007) find that equilibrium is more fragile with more players, as the first firm to raise its price may abandon it altogether, if it waits too long for others to follow suit. Also, their price-cutting Edgeworth cycles reduce profits — opposite to our cycles.

Roadmap. The next section introduces a parametric family of timing games in normal form, based on ASP. It notes key features of the Nash equilibria, called rushes and gradual play, as well as generalizations of wars of attrition and of preemption, called greed and fear. Section 3 presents our simulation procedures and shows how cycles emerge. Section 4 then lays out the laboratory experiment's procedures and design. It concludes with numerical predictions and general hypotheses to be tested. Experiment results are collected in Section 5, with a descriptive overview followed by test results for each hypothesis. A concluding discussion in Section 6 summarizes the main results and their wider implications, and suggests directions for future research. Appendix A collects mathematical details for the normal form game, and online Appendix B is a copy of instructions to experiment subjects.

2. Static model

A continuum of identical risk neutral players each choose a location $x \in [0, \infty)$. Location can be interpreted as a price, a leverage level, a physical location, etc., but borrowing from ASP we often will favor language that suggests interpreting x as a stopping time; see Table 1.

Each player's payoff $\pi(x, q)$ depends on x and also on its quantile $q = Q(x)$, i.e., on where the chosen location x fits into the cumulative distribution function (cdf) Q. Recall that $Q(x) \in [0, 1]$ is the fraction of players choosing $x' \leq x$. Recall also that the *support* of Q is the (closure of the) points of increase, where either the density $Q'(x)$ is positive (called gradual play in Table 1) or else Q is discontinuous (called a rush) indicating that a positive mass of the player population chooses exactly the same location.

Anderson et al. (2017) explore a general class of payoff functions $\pi(x, q)$. Here we focus on a fully solvable parametric family where payoffs are a product, $\pi(x, q) = u(x)v(q)$, and both factors are quadratic. We refer to $u(x)$ as the *fundamental factor* and assume that it takes the form $u(x) = 1 + 2\lambda x - x^2$, with parameter $\lambda > 0$. As illustrated in Fig. 2, u peaks uniquely at what we call the *harvest time* $\hat{x} = \lambda$; that maximal value is $u(\hat{x}) = 1 + \lambda^2$. To ensure that the fundamental factor is positive, we restrict location to $x \in [0, x_{max})$, where $x_{max} = \lambda + \sqrt{1 + \lambda^2}$.

For given parameters $\gamma > 1$ and $\rho > 0$, the *quantile factor* $v(q) = (1 - q/\gamma)(1 + q/\rho)$ is positive for all $q \in [0, 1]$. Note that $v(q)$ is maximized at the quantile peak $\hat{q} = (\gamma - \rho)/2$. Of course, as a quantile, q is defined only on the interval $[0, 1]$. Hence $v(q)$ monotonically decreases on $[0, 1]$ when $\gamma \leq \rho$, and monotonically increases when $\gamma \geq \rho + 2$. As illustrated in Fig. 1, it is hump-shaped when $\rho < \gamma < \rho + 2$.

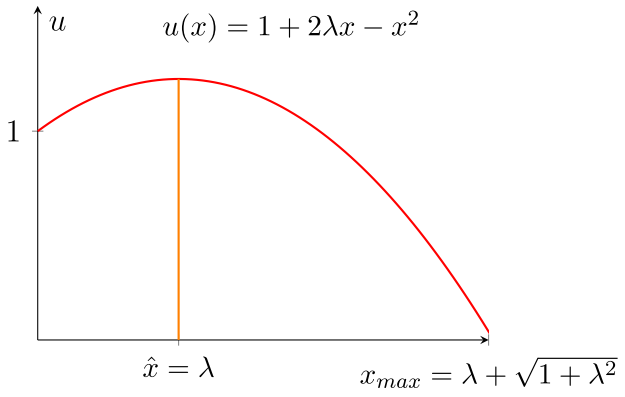

Fig. 2. Fundamental Factor Plot.

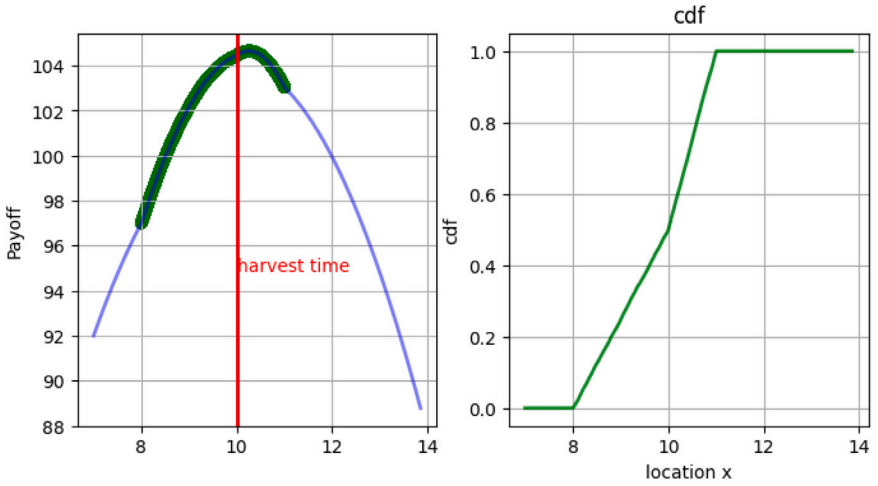

Fig. 3. Landscape and cdf: An Example. The cumulative distribution function Q (right panel) is arbitrarily chosen to have twice the density on $[10, 11]$ as on $[8, 10]$. The corresponding landscape $\pi(x, Q(x))$ for parameters $\lambda = 10, \rho = 3, \gamma = 4.4$ (left panel) peaks at $x^* \approx 10.5$, just above the harvest time $\hat{x} = 10$. Players' payoffs are in dark green, while blue line shows payoffs at locations not chosen in the given Q.

Fixing the cdf Q, the *payoff landscape* is the function $\pi(x, Q(x)) = u(x)v(Q(x))$. See Fig. 3 for an example. Note that, for a given distribution of the population of other players, increasing x shifts both one's fundamental factor $u(x)$ and quantile factor $v(Q(x))$. We will see in the next subsection these shifts offset each other in equilibrium.

2.1. Nash equilibrium

A *Nash equilibrium* for the payoff function $\pi(x, q)$ is a cumulative distribution (or quantile) function $q = Q(x)$ whose support contains only points with maximal payoff. That is, Q is a NE if $x \in supp(Q) \implies \pi(x, Q(x)) \geq \pi(y, Q(y))$ for all $y \geq 0$.

ASP note that there are Nash equilibria with all players coordinating on a common location x, but that these are fragile and not robust to the slightest location mistakes. Their focus (and ours) therefore is on "safe" Nash equilibria, which are not fragile in that sense.

Nash equilibria Q have distinctive landscapes. The equal maximal payoff property of NE implies that the landscape must consist of flat plateaus (over intervals of gradual play) and/or peaks (at rushes), all at the same altitude, representing the maximal payoff. Fig. 4 below shows examples of such landscapes.

On a gradual play plateau, players earn the same maximal payoff

$$\bar{w} = u(x)v(Q(x)) \tag{1}$$

for all x in the support of the NE. Differentiating (1) yields

$$0 = u(x)v'(Q(x))Q'(x) + u'(x)v(Q(x)), \tag{2}$$

so $Q'(x) = -u'(x)v(Q(x))/[v'(Q(x))u(x)]$. Since the density $Q'(x)$ is always positive with gradual play, and since both factors $u(x)$ and $v(q)$ are positive, the slope signs $v'(q)$ and $u'(x)$ must mismatch in any gradual play interval.

Following ASP, we refer to the case $u'(x) > 0 > v'(q)$ as *fear* (of missing out), since one's rank order is falling in q and thus in x. It is a local preemption game in that time passage is fundamentally beneficial but strategically costly. We refer to the other possible case $u'(x) < 0 < v'(q)$ as *greed*. In ASP, this referred to the oft-repeated idea that individuals hold out in a war of attrition driven by the greed for higher rank payoffs. It is local war of attrition in that time passage is fundamentally harmful but strategically beneficial.

2.2. Numerical examples

We shall now see that all four possible combinations of fear and greed, and of gradual play and rushes, arise in the safe Nash of our parametric family $u(x)v(q) = (1 + 2\lambda x - x^2)(1 - q/\gamma)(1 + q/\rho)$. Fix $\lambda = 10$ and $\rho = 3$. As the parameter $\gamma > 1$ rises, we shift from fear to greed, with pure gradual play equilibria at the beginning and end, while the middle case entails both fear and greed. To spell this out,

- First consider $\gamma \in (1, 3]$. As illustrated in Panel (a) of Fig. 4 with $\gamma = 2$, the only safe Nash equilibrium is a slow preemption game (fear) with support $[\underline{x}, 10]$. The top part of that panel shows that the maximum payoff ($\approx$ 67) is achieved by all players in the support interval (where $\underline{x} \approx 4$) and the landscape indicates lower payoffs outside that high plateau. Along the plateau, an increasing fundamental factor balances the decreasing quantile factor, exemplifying fear of missing out. Nash equilibrium requires a particular distribution Q on the support (illustrated in the bottom part of the panel) to make that balance perfect. Appendix A shows that other values of $\gamma \in (1, 3]$ yield a similar picture. The NE support interval begins at $\underline{x} = 10 - \sqrt{101}\sqrt{1 - \frac{64(\gamma-1)}{3(\gamma+9)(\gamma+1)}}$, and ends at the harvest time $\hat{x} = \lambda = 10$; see Eq. (9) and surrounding discussion for more general formulas.
- For $\gamma \in (3, 3 + 2/3]$, the unique safe Nash is a rush of mass $q_0 = 0.75(\gamma - 3)$ at the lower endpoint $\underline{x}$, followed by gradual play over the rest of the support interval. Fig. 4 Panel (b) illustrates for $\gamma = 3.6$: the cdf in the lower part shows a jump at $\underline{x} \approx 8$ of $q_0 = 0.75(0.6) = 0.45$, i.e., 45% of the population chooses exactly the same location $\underline{x}$, and the remaining 55% choose locations between there and the harvest time $\hat{x} = \lambda = 10$. The decreasing density (concave cdf) of gradual play over the support interval enables the deteriorating quantile factor to perfectly offset the improving fundamental factor, as in preemption games (or fear). See Eq. (4) in Appendix A for an explicit formula covering this case.
- For $\gamma \in (3 + 2/3, 3 + 4/3)$ there are two NE. One is the same sort of equilibrium as before: fear with a rush q_0 at $\underline{x}$ followed by slow play on $[\underline{x}, 10]$. The other (safe) Nash equilibrium is different. It can be described as a post-harvest time greed over the interval $[10, \bar{x}]$, ending in a rush. Appendix Eqs. (6) and (14) show that the fraction of the population involved in the final rush is $1 - q_1$, where $q_1 = \frac{3\gamma-11}{4}$, and it occurs at location $\bar{x} = 10 + \sqrt{101}\sqrt{1 + \frac{48\gamma}{(3\gamma-11)(\gamma-1)}}$. This case is not illustrated in Fig. 4.
- For $\gamma \in [3 + 4/3, 5]$ there is only one safe Nash as just described: greed (a post-harvest time war of attrition) ending in a rush of size q_1 at $\bar{x}$, as illustrated in Fig. 4 Panel (d).
- For $\gamma \geq 5$, the only safe Nash is a pure post-harvest time slow war of attrition (greed), over the interval $[10, \bar{x}]$, as illustrated in Fig. 4 Panel (c).

3. Simulations of tâtonnement dynamics

The last section showed that our location games have a distinctive set of (safely robust) Nash equilibria, including both rushes and gradual play. The equilibria assume a continuum of maximizing agents who correctly anticipate the location distribution.[5]

Do those equilibria usefully predict behavior that we might observe in a finite world of imperfect rationality? To address that question, we run the human subject experiment described in Section 4 below. It is not immediately obvious how long to run the experiment to allow convergence, nor what are appropriate choices of payoff parameters, number of players, etc. It is also helpful to have alternative hypotheses beyond quick appearance of Nash equilibrium.

For guidance, we supplement the static theory summarized in the previous section by dynamic computer simulations with a finite number of identical boundedly rational agents (*bots*) who follow a simple myopic adjustment procedure. The dynamic simulations help us parametrize the experiment and enrich the set of testable hypotheses.

3.1. Simulation procedures

Our simulations take place on a fine grid of locations $x = 0, 0.01, 0.02, \ldots, 99.98, 99.99, 100$. At time $t = 0$, each of a set of bots (automated agents $i = 1, \ldots, N$) is assigned an initial location $x_{i,0}$ on the grid. Some of the simulations reported below use $N = 20$ and others use $N = 1000$; they all use initial locations that form the best discrete approximation of the relevant safe Nash cdf. Other simulations, not reported below, obtained qualitatively similar results using random or uniformly spaced initial locations, different numbers of bots, and coarser grids.

At each subsequent time step $t = 1, 2, \ldots, T$, some bots are allowed to change their locations as follows.

[5] Since payoffs depend on other players' actions only via the resulting cdf, it is possible to show that these approximate all finite player and finite action games, for a fine enough action grid and large enough number of players. We omit the lengthy technical proof of this intuitive result.

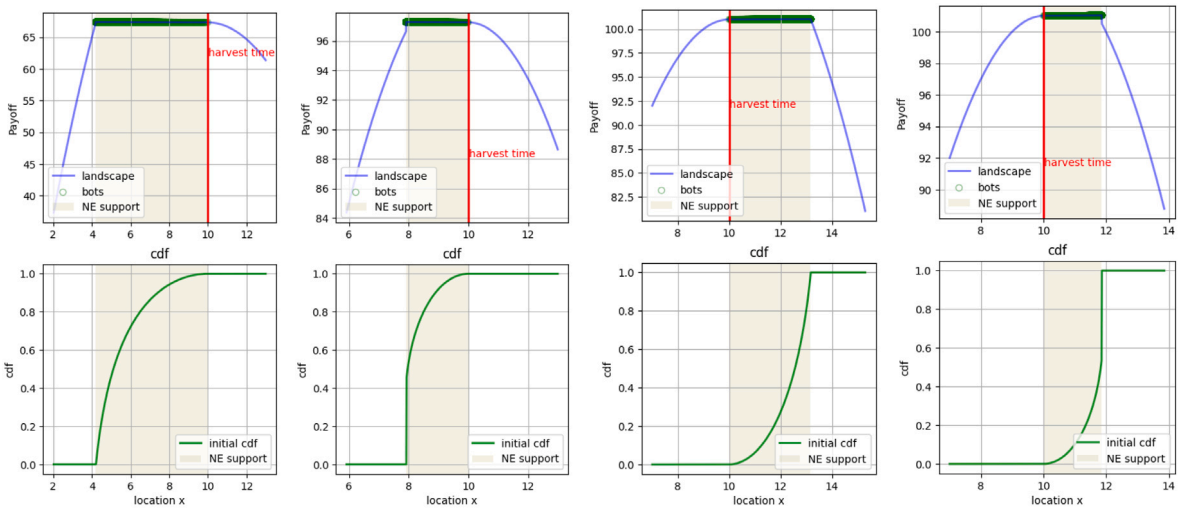

(a) fear without rush ($\gamma = 2$) (b) fear with rush ($\gamma = 3.6$) (c) greed without rush ($\gamma = 6$) (d) greed with rush ($\gamma = 4.4$)

Fig. 4. Nash equilibrium. Top row shows NE landscapes, bottom row shows NE cumulative distribution functions (green line) for the parametric model when $\lambda = 10, \rho = 3$. In Panels (a, b, c, d) respectively, the parameter $\gamma = 2, 3.6, 6, 4.4$.

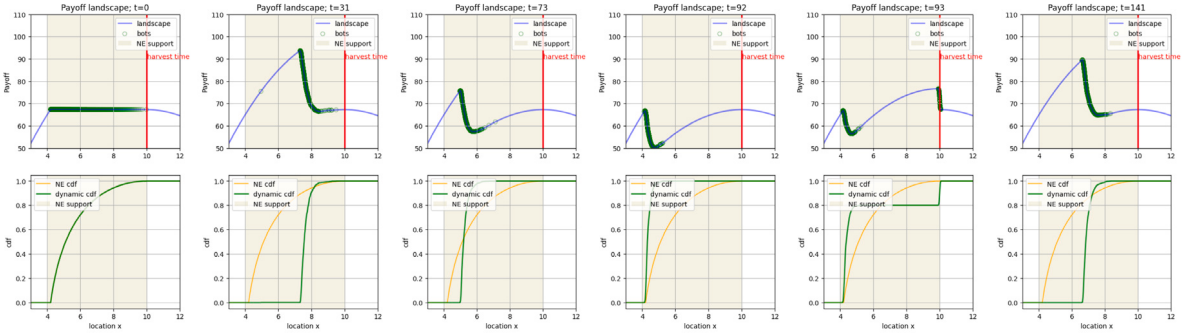

(a) phase 1 (b) phase 2 (c) phase 3 (d) phase 4 (e) phase 5 (f) phase 6

Fig. 5. Fear landscape and cdf dynamics in simulation with move fraction $g = 0.2$, noise amplitude $\sigma = 0.03$, $N = 1000$ bots and payoff parameters $\lambda = 10, \rho = 3$, and $\gamma = 2$; the safe Nash type is fear with no rush. Successive columns show the state at time steps $t = 0, 31, 73, 92, 93, 141$.

(1) *Computing the Payoff Landscape*: Given the cdf $Q(x, t-1)$ of locations chosen in the previous time step, compute the landscape $\pi(x) = u(x)v(Q(x, t-1))$ at all grid points, and determine its maximum payoff π^* and the corresponding argmax (best payoff location) x^*.
(2) *Determining Who Moves*: A fraction g of the N bots is randomly selected to move, while the remaining players stay in their current locations: $x_{i,t} = x_{i,t-1}$.
(3) *Determining Where They Move*: The bots who move go to the best payoff location x^* offset by "tremble" noise. That noise is normally distributed $N(0, \sigma^2)$. The noise parameter $\sigma > 0$ helps prevent stagnation at an arbitrary point.

The number of time steps T is typically in the thousands. Other simulations, not reported below, obtained qualitatively similar results using different rules on who moves (e.g., precedence given to bots with lower current payoff) and on where they move (e.g., using a logit rule that allows bots to select a location far from x^* when its payoff is not far below π^*).

3.2. Emergent behavior

The most striking feature of our dynamic simulations is that they do not converge to NE, nor to any other fixed distribution. Instead, large cycles emerge, as illustrated in Figs. 5 and 6, for games with fear and greed equilibria. In these simulations, the initial bot locations closely approximate a safe Nash cdf, so their initial payoffs are almost the same and maximal, as shown in each figure's first subplot. After several periods, bots' choices begin to cluster tightly (second subplot). The cluster then drifts away from the harvest time $\hat{x} = 10$ (third subplot). This behavior continues until the payoff at the cluster drops below the payoff at $\hat{x} = 10$,

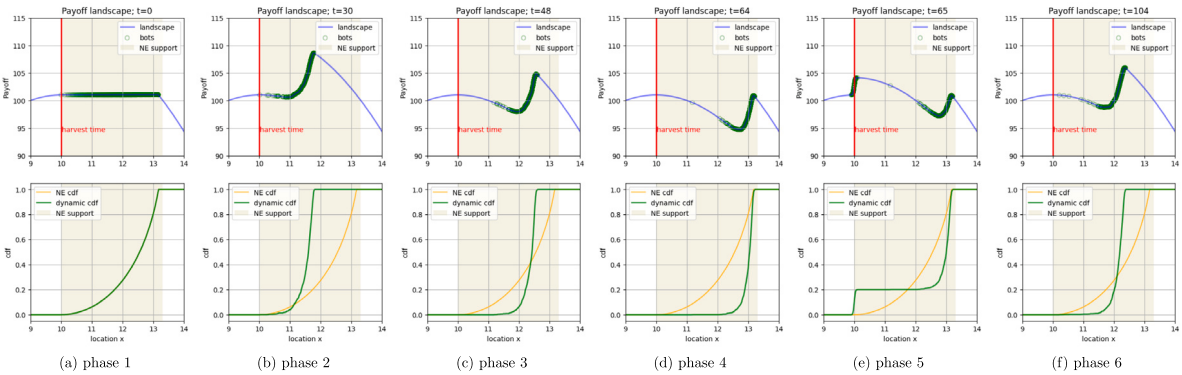

Fig. 6. Greed landscape and cdf dynamics in simulation with move fraction $g = 0.2$, noise amplitude $\sigma = 0.03$, $N = 1000$ bots and payoff parameters $\lambda = 10, \rho = 3$, and $\gamma = 6$; the safe Nash type is greed with no rush. Successive columns show the state at time steps $t = 0, 30, 48, 64, 65, 104$.

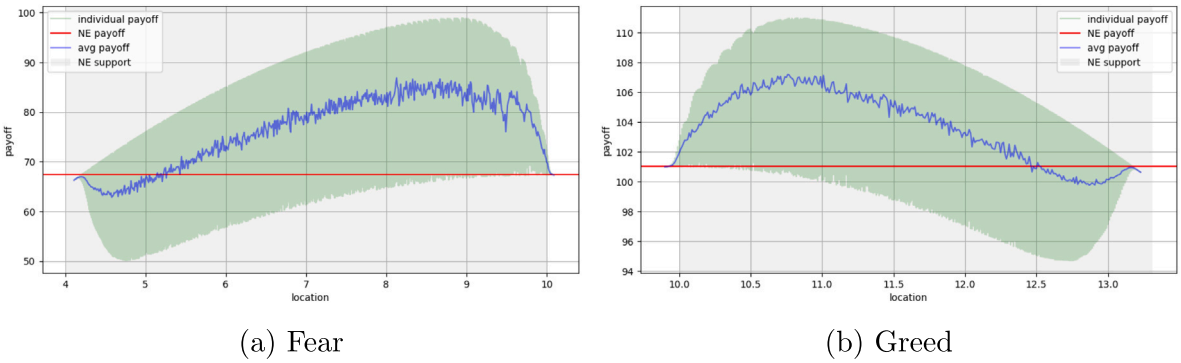

Fig. 7. Average payoff by location. Panel (a) shows average payoffs for Fig. 5 simulation and panel (b) for Fig. 6 simulation.

prompting the bots to jump back to near $\hat{x} = 10$ (fourth and fifth subplots). That process repeats (compare sixth and second subplots) until the time expires ($t = T$); the bot distribution never returns to the initial safe Nash pattern.

Fig. 7 shows that the average payoff in most locations is well above the Nash payoff, suggesting that the cyclical payoffs overall are strictly higher than the Nash payoff.

Fig. 8 illustrates cycles for the parameters we use in the experiment described below. As noted, similar cycles emerge in simulations with different leaving or arrival rules, different initial conditions and different payoff and adjustment parameters. Generally speaking:

- A cycle arises over an interval close to the safe Nash support interval, with upper (resp. lower) endpoint near the harvest time for fear (resp. greed).
- For payoff parameters yielding a safe Nash with fear, bots cluster near the harvest time $\hat{x}$ and then slowly move downward until they are near the lower support point $\underline{x}$. Bots then jump back up to near $\hat{x}$, and resume anew the downward movement.
- For parameters supporting a safe Nash with greed, an analogous cluster drifts upward, to the right of the harvest time, and jumps back to near $\hat{x}$ when it approaches $\bar{x}$.
- As in Fig. 7, average payoff over the cycle exceeds the safe Nash payoff, especially for parameters supporting a gradual fear equilibrium.
- As in Fig. 8, cycles seem to take longer (i.e., there are fewer cycles in a given number time steps) for the chosen payoff parameters that support larger rushes.
- Across the parameter ranges explored —— $N \in [20, 5000]$, $g \in [5\%, 80\%]$, and $\sigma \in [0, 0.5]$ ——cycles take longer as N decreases (fewer bots), as g decreases (a smaller fraction of bots can move each round), and as σ decreases (lower noise amplitude). Despite these changes in cycle length, the qualitative patterns of cycle emergence and persistence remain unchanged.

4. Experiment

Does the static model or the simulated adaptive dynamics (or neither) usefully describe how finite human populations play location games? To investigate, we ran a laboratory experiment.

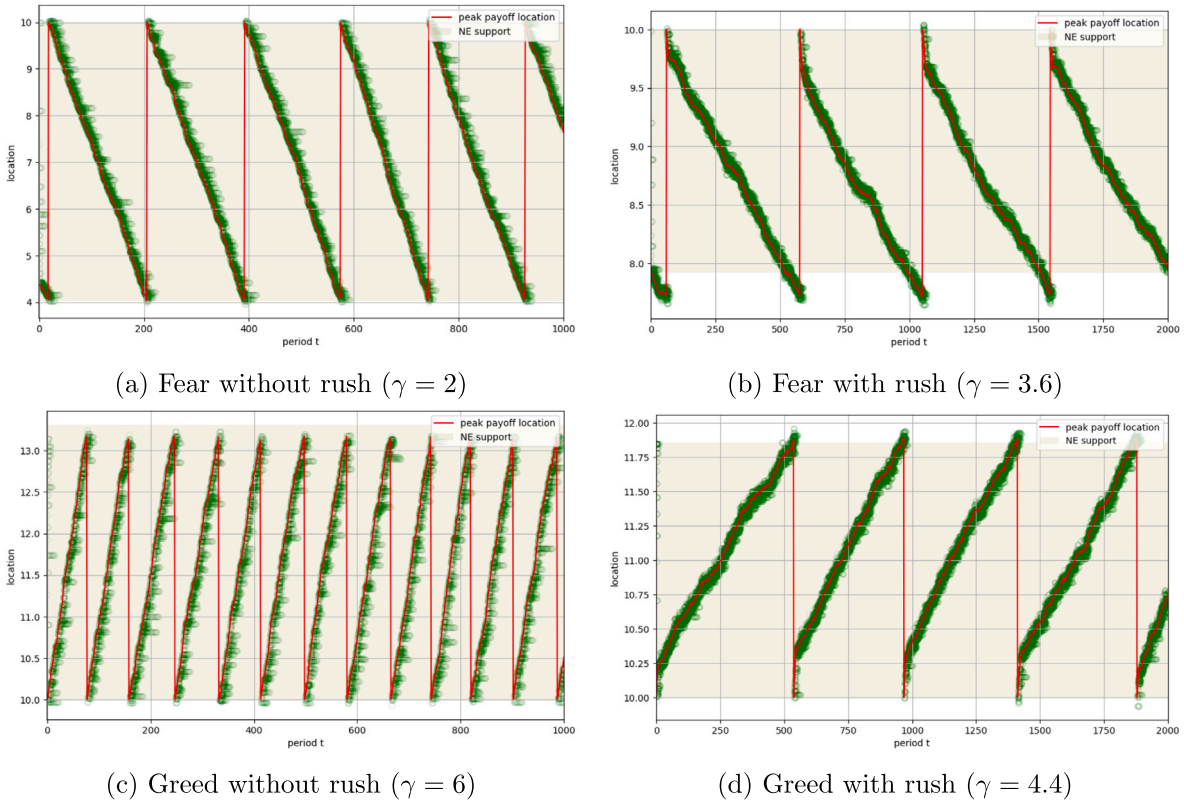

Fig. 8. Location Dynamics in Simulations. Individual locations x_i (green lines) for $N = 20$ bots and best payoff location x^* (red) are plotted over $T = 1000$ time steps (or, for better clarity in panels (b) and (d), $T = 2000$) in simulations using payoff parameters $\lambda = 10, \rho = 3$, and the γ values noted in Panels (a–d). Light olive shading marks the safe Nash support interval.

4.1. Procedures

The location game is implemented by adapting oTree software (Chen et al., 2016). All participants in the experiment are undergraduate students at UC Santa Cruz, recruited through the online system ORSEE (Greiner, 2004) installed on the LEEPS lab website. In each session, participants first read a printed version of the instructions. The experimenter orally summarizes the basic rules. The participants then form a single group (or population) and play a series of rounds, each lasting 150 s.[6] The first two rounds are for practice (unpaid), and questions are encouraged. Then 16 paid rounds are conducted for data collection.

Participants are guaranteed a show-up fee of $6. One of the 16 rounds is randomly selected for actual payment. The accumulated payoff for that round is calculated, and any payoffs exceeding a given threshold are converted into US dollars. Payment details are given in the instructions and each participant sees the personal calculation on her own final screen. The experimenter makes cash payments via Venmo or Zelle. The average payment across all sessions is $23.58, with a standard deviation of $2.68.

In each period, players (the human participants) interact via a screen, as illustrated in Fig. 9. Key features include the following.

- The large *Landscape Plot* on the left displays the payoff rate at all possible locations along the horizontal axis during the current time step. The green diamond marker indicates the player's current location, while small circles represent the locations of the other players. The player can move the cursor to see the payoff rate at any other location, and can click there to change location. The text and fill bar above indicate the update latency (3.0 s in Fig. 9 but 0.5 or 1.0 s in paid rounds) and time remaining in the current time step.
- The *Position History Plot* at top right displays the history of location choices for all subjects so far in the current round.
- The *Payoff History Plot* at bottom right similarly tracks the player's own payoff and the group's average payoff so far in the current round.

[6] As detailed below, successive rounds within a block represent stationary repetition, the traditional way to test equilibrium predictions in experiments since Smith (1962).

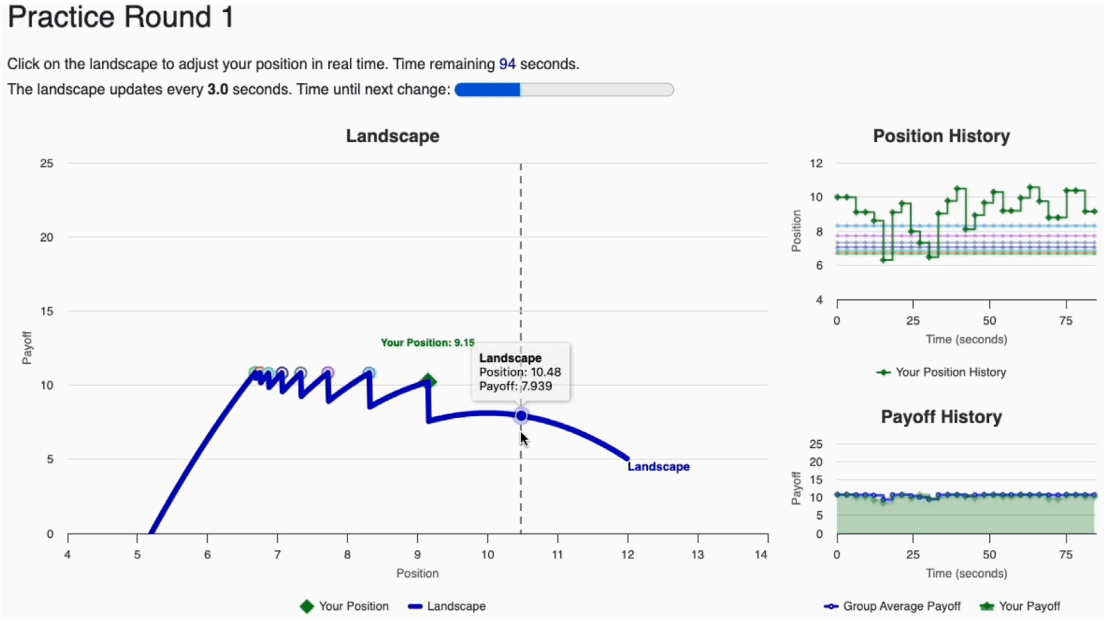

Fig. 9. Game Interface.

Table 2
Session design. N is the number of humans in the population, and latency is the length of a time step (for refreshing screens and recording locations). Blocks are 4 rounds each. Greed (resp. Fear) is supported by parameters $\gamma = 4.4, 6$ (resp. $\gamma = 2, 3.6$) and Rush (resp. NoRush) by $\gamma = 3.6, 4.4$ (resp. $\gamma = 2, 6$).

Session #	N	latency	Round	Parameter (γ)			
		(in seconds)	(in seconds)	Block 1	Block 2	Block 3	Block 4
1	11	1	150	2	3.6	6	4.4
2	12	0.5	150	2	3.6	6	4.4
3	11	0.5	150	4.4	6	3.6	2
4	10	1	150	4.4	6	3.6	2

At the start of each round, players are randomly assigned initial locations within a discrete approximation of the NE, given the payoff parameters set for that round. At later time steps, players adjust their location by clicking on the landscape plot. Multiple clicks within a time step are allowed, but only the last click before the time step ends is recorded as the location for that time step. Players can make further adjustments during the next time step.

Payoffs are determined as in the parametric model in Section 2. Algebraic expressions are not shown to players, but they see the resulting landscape and are told that payoffs depend only on their own location and the locations of other participants. We scale the payoff range to ensure it falls between 0 and 25 in all treatments. This normalization roughly equalizes the monetary incentive intensity across treatments.

4.2. Design

The experiment consists of 4 sessions, conducted in February and March 2025, each involving 10–12 human participants interacting within a single group. Each session is divided into 4 blocks, with each block containing 4 rounds. Treatment parameters vary across blocks but remain constant within each block. The order of blocks is reversed across different sessions.

Table 2 summarizes the design, which can be described as 2×2 factorial within-session with replication index (blocksize) 4, where the payoff parameter γ defines the fear vs greed factor as well as the rush vs no-rush factor. Between sessions the design is 2×2 factorial with replication index 1; here the factors are nuisance variables: the block sequence and the latency (time step interval) at 0.5 or 1 s. The design is intended to enable examination of each parameter configuration in four independent sessions, while ensuring that results do not depend on a single fortuitous configuration of nuisance variables.

Table 3
Predictions. Payoff function parameters are $\lambda = 10, \rho = 3$, with γ as in first column. Nash equilibrium predictions for rush size appear in the second column, and for rush location (in **bold** font) in the third column; slow play is predicted within the Support interval. NE payoff predictions appear in the fourth column. Remaining columns show cycle predictions based on simulations with $N = 20$ bots, $g = 0.20$ (i.e., 4 random leavers) per time step, and best response arrival with $N(0, 0.03^2)$ tremble. Length is relative to $\gamma = 2$ (180 time steps). Domain interval is from the first percentile to 99th percentile of realized bot locations, and Payoff/NE reports overall mean payoff relative to the corresponding safe Nash payoff.

	Static prediction: NE			Dynamic prediction: Cycle		
γ	Rush	Support	Payoff	Length	[.01, .99] Domain	Payoff/NE
2	0	[4.02, 10]	67.33	1	[4.07, 9.96]	1.13
3.6	0.45	[**7.92**, 10]	97.26	2.75	[7.73, 9.84]	1.01
4.4	0.45	[10, **11.86**]	101	2.48	[10.18, 11.89]	1.01
6	0	[10, 13.31]	101	0.46	[10.02, 13.16]	1.03

4.3. Testable hypotheses

The experiment explores the explanatory power of static theory (the safe Nash equilibria) and of adaptive dynamics. Table 3 summarizes the numerical predictions. To focus our exploration, we test six hypotheses.[7]

Hypothesis 1. Consistent with both static theory and dynamic simulations, over 90% of observed actions in each treatment will be in the safe Nash support interval. Also, over 90% of actions x in the Fear (resp. Greed) treatments will satisfy $x < 10.1$ (resp. $x > 9.9$).

Hypothesis 2. Consistent with dynamic simulations but inconsistent with static theory, the overall distribution of observed actions in each treatment will be closer to the uniform than to the safe Nash distribution according to standard Kolmogorov–Smirnov statistics.

Hypothesis 3. Consistent with dynamic simulations but inconsistent with static theory, we will see cycles initiate at least 3 times per round on average in each treatment.

The next hypothesis is that we will see lots of small downward changes in location with fear, balanced by a few large upward changes, and will see the reverse with greed. To quantify that idea, the hypothesis uses the notation $\Delta x = x_t - x_{t-1}$ for location changes by a player (index i suppressed) in a given time step t, and $\#N$ (resp. $\#P$) for the number of location changes across all individuals within a round that are negative (or downward, $\Delta x < 0$) (resp. are positive or upward, $\Delta x > 0$). Finally, $\mu_N = \mu_N(\{|\Delta x|\})$ denotes the mean (absolute) size of the $\#N$ negative location changes, while $\mu_P = \mu_P(\{|\Delta x|\})$ is the mean size of the $\#P$ positive location changes.

Hypothesis 4. Consistent with dynamic simulations but inconsistent with static theory, the distribution of individual location changes Δx will differ significantly from any symmetric distribution in each treatment. In particular, $\#N > \#P$ but $\mu_N < \mu_P$ for $\gamma < 4$ (fear) treatments, and both inequalities will be reversed for the $\gamma > 4$ (greed) treatments.

Hypothesis 5. Consistent with dynamic simulations, average cycle lengths for rush treatments $\gamma = 3.6$ and 4.4 will be significantly longer than for no-rush treatments $\gamma = 2$ or 6.

Hypothesis 6. Consistent with dynamic simulations, the ratio of average actual payoff to safe Nash payoff will exceed 1 in all treatments.

5. Experiment results

We begin with data overviews and summaries. They will orient the reader and help motivate the test statistics used in Section 5.2.

5.1. Descriptive statistics

Fig. 10 plots all individual human player location choices over time for one sample round from each equilibrium type. In each of the rounds shown, one sees cycles roughly similar to those obtained in simulations: players tend to clump together, and most of the time the clump slowly moves away from the harvest time (location $\hat{x} = 10$, plotted on the vertical axis). When the clump reaches the far end of the safe Nash support interval (or often somewhat earlier) players jump back towards $x = 10$, sometimes stopping

[7] We pre-registered these hypotheses at https://archive.org/details/osf-registrations-csjm6-v1 before running any of the sessions described above. The pre-registered hypotheses are lightly edited here for clarity; the only substantive change is that we omit predictions for $\gamma = 4$ treatments, which, for reasons alluded to in Section 6, we have not yet run.

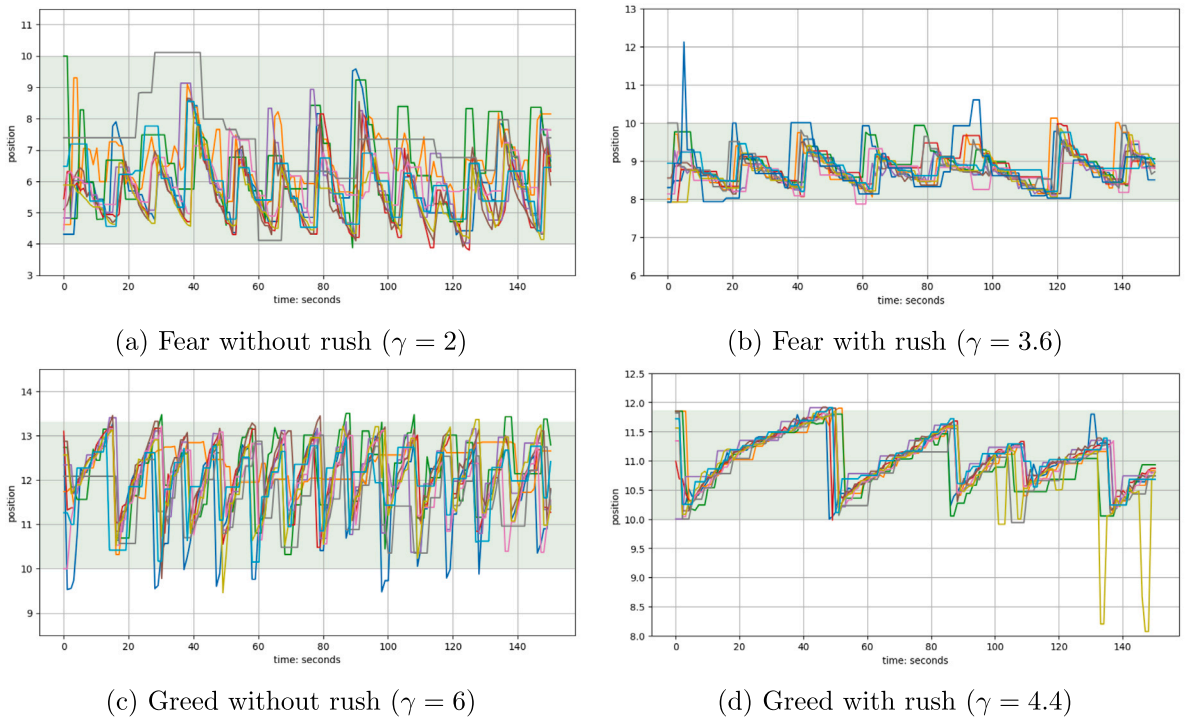

Fig. 10. Location Dynamics. Individual locations x_i are plotted over time in selected rounds: (a) session 4, round 13; (b) session 1, round 6; (c) session 4, round 5; and (d) session 4, round 1. Each color represents the trend of a different subject's locationover time. Light green shading marks the safe Nash support interval.

short but seldom jumping much beyond it. (The sole exception shown is the olive player in panel (d) who jumps down almost to 8 at times $t \approx 130, 150$ but quickly jumps back up to 10 or 11.) There are more cycles in panels without NE rushes — almost a dozen each in panels (a) and (c) — than in the NE rush panels — about half a dozen in (b) and (d).

Fig. 11 shows realized payoffs by location for the same sample rounds. Although average realized payoffs (blue line) can fall below the safe Nash level (horizontal dashed red line) near the far end of the support interval, they are usually well above that level. In all four panels, the realized payoff averaging over all chosen locations (black dashed line) exceeds the safe Nash payoff.

Roughly similar behavior appears in most of the other 60 rounds not shown here. Sometimes the cycles are more ragged, and often one or two players linger in a seemingly arbitrary location. A minor example of such behavior is the gray player in panel (a), who lingers near $x = 10.1$ for $t \in (27, 43)$. The overall average realized payoff lies consistently above the safe Nash level.

A more systematic analysis of cycles requires an operational definition. Reasonable observers might differ as to whether, e.g., panel (b) of Fig. 10 shows 7 cycles or 8. Somewhat arbitrarily, we deem a cycle to be complete at time step t when, in the last 5 s, at least 40% of players moved at least 25% of the Nash support width towards $\hat{x}$ in a single step. The number of cycles observed in a given period is the number of such completions.

That operational definition seems to capture intuitive impressions reasonably well for the sample periods shown, which all use latency (time step interval) of one second. One might wonder about the comparability of sessions with half second latency. Fig. 12 offers some reassurance. It shows that on average 20%–30% of players change location (by any amount) each time step with latency 0.5, versus 40%–50% with one second latency, with little or no within-period trend. So per-second mobility seems roughly similar across the latency treatments.

Table 4 summarizes key aspects of observed behavior in our experiment. It shows that the average number of cycles per round is a bit more with half-second than with 1 s time steps, and that the quantile factor parameters with no rush equilibrium ($\gamma = 2, 6$) tend to produce more cycles than those with a rush equilibrium ($\gamma = 3.6, 4.4$). As hypothesized, the payoff ratios are all above 1.0, especially those for $\gamma = 2$. As just noted, Move Percent (per time step) responds to latency, but it seems not to respond appreciably to the types of safe Nash (γ) treatments. Observed cycle domains seem to match up well with those obtained from simulations, which in turn match up with the safe Nash support intervals.

5.2. Test results

We now review the evidence for each of our testable hypotheses.

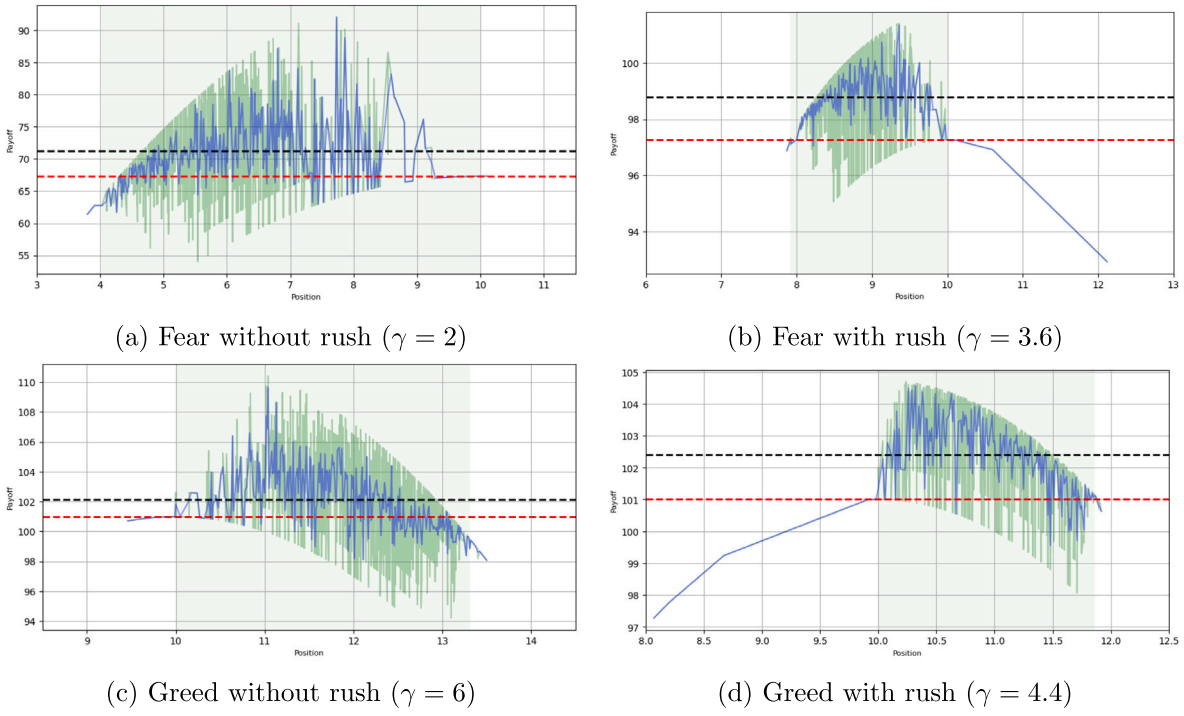

(a) Fear without rush ($\gamma = 2$)

(b) Fear with rush ($\gamma = 3.6$)

(c) Greed without rush ($\gamma = 6$)

(d) Greed with rush ($\gamma = 4.4$)

Fig. 11. Payoff by location. Selected rounds are the same as in Fig. 10. The green lines indicate individual payoffs and the blue line shows the average payoff for each location. Ratios of realized to Nash payoffs (dashed black/dashed red lines) are 1.057, 1.016, 1.011 and 1.014 in panels (a–d), indicating that here actual payoffs exceed equilibrium payoffs. The shaded area indicates the safe Nash support interval.

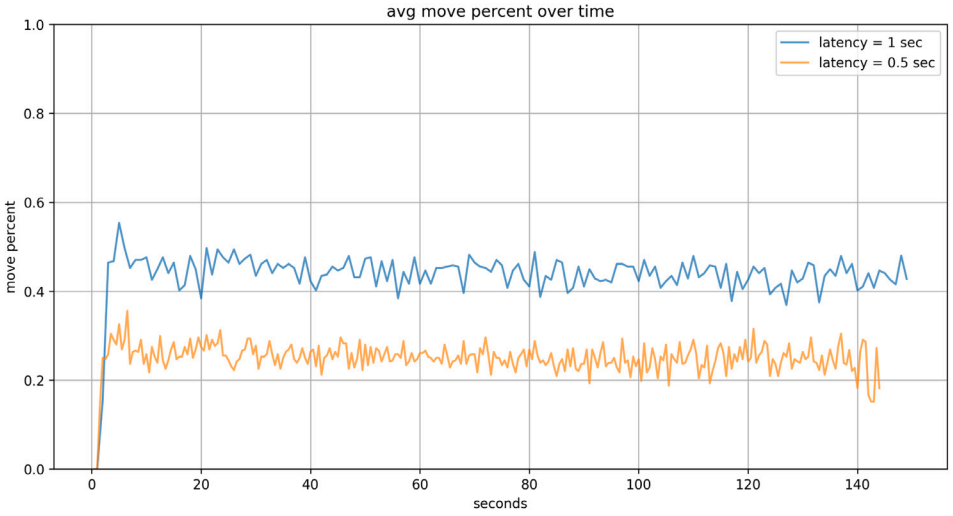

Fig. 12. Move Percent over Time. The fraction of players that move at each time step is shown, averaged over all sessions with given latency. Latency is the time step interval, i.e., length of time step. Most players so do not move with either latency. Naturally, fewer move each period with half second than one second latency.

Result 1. *Hypothesis 1 is confirmed. Observed actions reliably fall in the predicted intervals.*

Table 5 shows that over 90% — indeed, usually well over 95% — of observed actions in each treatment are on the predicted side of the harvest time (with 0.1 leeway) and are in the safe Nash support interval. According to conventional tests, the difference from the hypothesized 90% is very highly significant. (The significance levels indicated here and below should be taken with a grain of salt, since the conventional tests assume that all observations are independent. Actual dependence among observations may reduce significance levels but not change the point estimate, e.g. 95.6% indeed exceeds 90%.)

Table 4
Means of observed variables (standard deviations in parentheses). Cycles/Round is the number of completed cycles in a round. Payoff Ratio is average actual payoff in a round divided by safe Nash payoff. Move Percent is the fraction of players changing location at each time step within a round. Cycle Domain indicates the central 98% confidence interval for location, from the first to the 99th percentile of all locations observed at each time step in a period, after removing outliers (values more than 5% beyond the harvest time).

	Cycles/Round	Payoff ratio	Move percent	Cycle domain
Latency 0.5 s				
fear without rush ($\gamma = 2$)	10.250	1.067	0.243	[4.29, 10.33]
	(0.886)	(0.023)	(0.127)	
fear with rush ($\gamma = 3.6$)	8.375	1.014	0.225	[7.92, 10.26]
	(2.264)	(0.005)	(0.125)	
greed without rush ($\gamma = 6$)	10.500	1.011	0.290	[9.80,13.36]
	(2.070)	(0.002)	(0.130)	
greed with rush ($\gamma = 4.4$)	9.625	1.009	0.240	[9.92,11.85]
	(2.560)	(0.002)	(0.137)	
Latency 1 s				
fear without rush ($\gamma = 2$)	8.750	1.057	0.459	[4.10,9.75]
	(1.982)	(0.038)	(0.177)	
fear with rush ($\gamma = 3.6$)	7.250	1.013	0.411	[7.80, 9.99]
	(1.165)	(0.004)	(0.171)	
greed without rush ($\gamma = 6$)	7.250	1.008	0.477	[10.01,13.32]
	(1.165)	(0.006)	(0.167)	
greed with rush ($\gamma = 4.4$)	6.500	1.012	0.424	[9.93,11.85]
	(0.756)	(0.002)	(0.172)	

Table 5
Test of Hypothesis 1. Standard errors in parentheses. The classic one sample z test with null hypothesis that the proportion is 0.9 has p-values indicated by * for $p < 0.1$, ** for $p < 0.05$, and *** for $p < 0.01$. Observations are treated as independent within each group, but standard errors are clustered at the session level to account for correlation within sessions.

	Proportion within safe Nash support	Proportion that $x < 10.1$ for fear or $x > 9.9$ for greed	Sample size
Latency 0.5 s			
fear without rush ($\gamma = 2$)	0.956**	0.963***	25 497
	(0.027)	(0.025)	
fear with rush ($\gamma = 3.6$)	0.949***	0.964***	25 651
	(0.002)	(0.001)	
greed without rush ($\gamma = 6$)	0.949***	0.981***	25 735
	(0.018)	(0.003)	
greed with rush ($\gamma = 4.4$)	0.974***	0.990***	25 939
	(0.002)	(0.003)	
Latency 1 s			
fear without rush ($\gamma = 2$)	0.986***	0.996***	12 813
	(0.006)	(0.002)	
fear with rush ($\gamma = 3.6$)	0.962**	0.995***	12 684
	(0.027)	(0.000)	
greed without rush ($\gamma = 6$)	0.979***	0.993***	12 662
	(0.005)	(0.002)	
greed with rush ($\gamma = 4.4$)	0.980***	0.990***	12 629
	(0.004)	(0.002)	

Given that observed actions fall into the correct intervals, we now consider which prediction better describes the distribution over that interval. For each parameter controlling fear/greed and rush/no-rush ($\gamma = 2, 3.6, 4.4, 6$), Fig. 13 shows the cdf of all observations in our experiment (green curve) together with three benchmarks: the cdfs of the safe Nash (blue curve), the uniform distribution on the safe Nash support interval (black dashes), and the time-average of the adaptive dynamic simulations as specified in Table 3 (orange curve). The simulated dynamics produce a location distribution that is very nearly uniform in all four cases, and in the no-rush cases ($\gamma = 2, 6$) the support intervals closely coincide. The empirical distribution is not very close to uniform, but neither is it particularly close to the safe Nash distribution. The empirical cdf seems best approximated by the simulated dynamic cdf in the greed/Rush case, but in general the empirical distribution has less mass near the harvest time ($\hat{x} = 10$). That feature brings it closer to the safe Nash cdf in that part of location space, but the empirical cdf is far from safe Nash in the more distant part of its support (near $\bar{x}$ for greed, near $\underline{x}$ for fear).

For a more quantitative assessment, we use the Kolmogorov–Smirnov test statistic, a standard measure of the distance between two cdf's. The relatively small numbers in last row of Table 6 confirms the impression from Fig. 13 that the simulation cdf is relatively close to the uniform cdf on the safe Nash support interval. Comparing the first two rows of the Table for the rush treatments ($\gamma = 3.6, 4.4$), we see that the overall distribution of observed actions ("Empirical") is noticably closer to the simulation cdf than to the safe Nash cdf according to these tests, but it is about equidistant for no-rush treatments ($\gamma = 2, 6$). In sum:

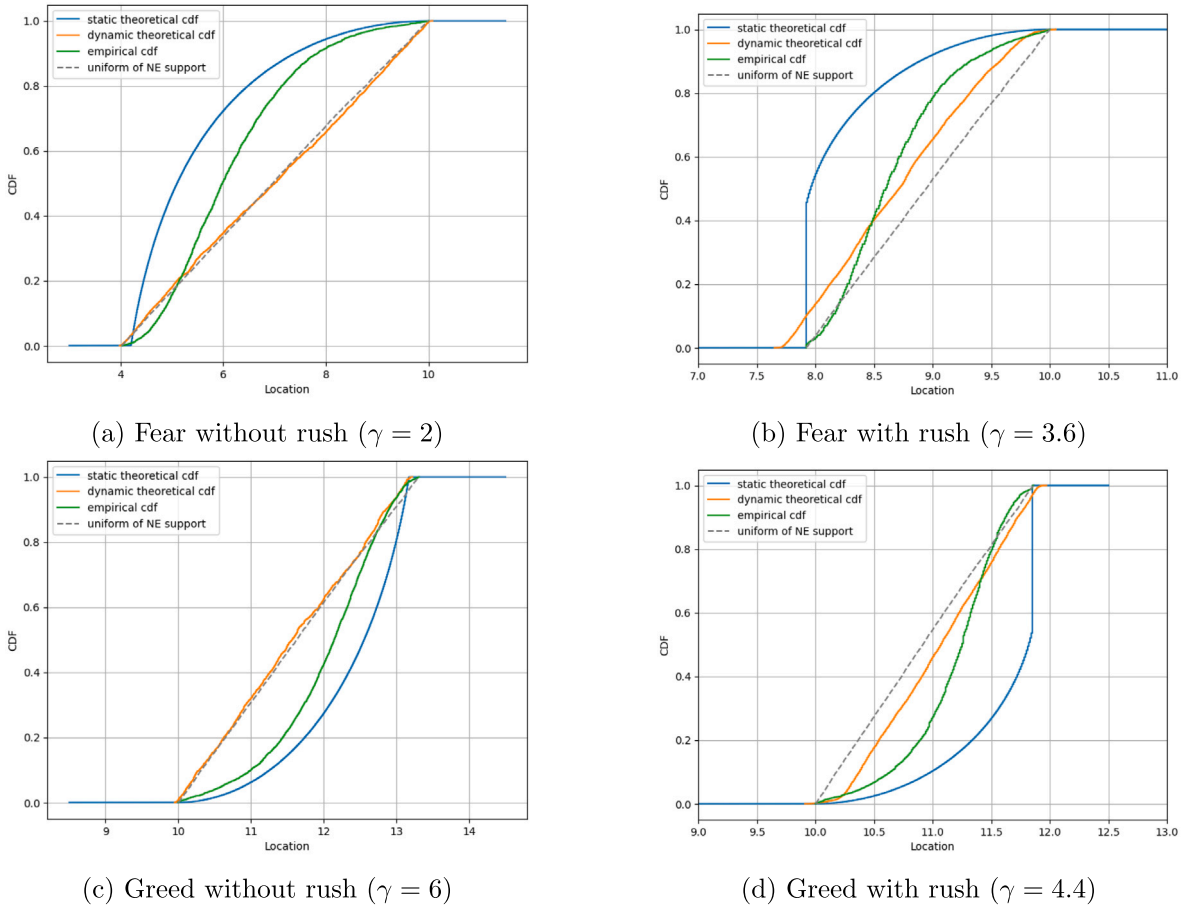

Fig. 13. Cdf Comparison. The static theoretical (safe Nash) cdf is the blue curve. The dynamic theoretical cdf (orange) is from simulations with $N = 20$ bots, each completing at least 3 cycles; each simulation is repeated with four random seeds. The empirical cdf (green) is obtained by sampling once per second from each relevant human subject round. The dashed line represents a uniform distribution over the safe Nash support interval.

Table 6
Kolmogorov–Smirnov test statistics associated with cumulative distribution functions in Fig. 13. $^{*}p < 0.1;^{**}p < 0.05;^{***}p < 0.01$.

	Kolmogorov–Smirnov Statistic			
	Fear without rush ($\gamma = 2$)	Fear with rush ($\gamma = 3.6$)	Greed without rush ($\gamma = 6$)	Greed with rush ($\gamma = 4.4$)
Empirical vs safe Nash	0.318***	0.553***	0.241***	0.569***
Empirical vs Simulation	0.280***	0.134***	0.263***	0.197***
Simulation vs Uniform	0.022***	0.133***	0.040***	0.110***

Result 2. *Hypothesis 2 is partly confirmed. According to KS statistics, the empirical cdfs are closer to the simulation cdfs than to the safe Nash cdfs for rush treatments, and no further away for the no-rush treatments. But locations close to $\hat{x}$ are much less frequent empirically than in the simulations.*

We now examine how observed human behavior changes within a period. We can clearly reject static models that predict that the action distribution settles down to safe Nash or to any other fixed distribution. Instead, using our operational definition of cycles (or presumably any other reasonable definition), persistent cycles arise in each treatment. Indeed, the first column of Table 4 shows that on average we have at least 6.5 cycles per period in each treatment, and the variance in the number of cycles is not especially high.

Result 3. *Hypothesis 3 is confirmed. The mean number of cycles per period ranges from 6.5 to 11.5 depending on the treatment, far in excess of the hypothesized 3.0.*

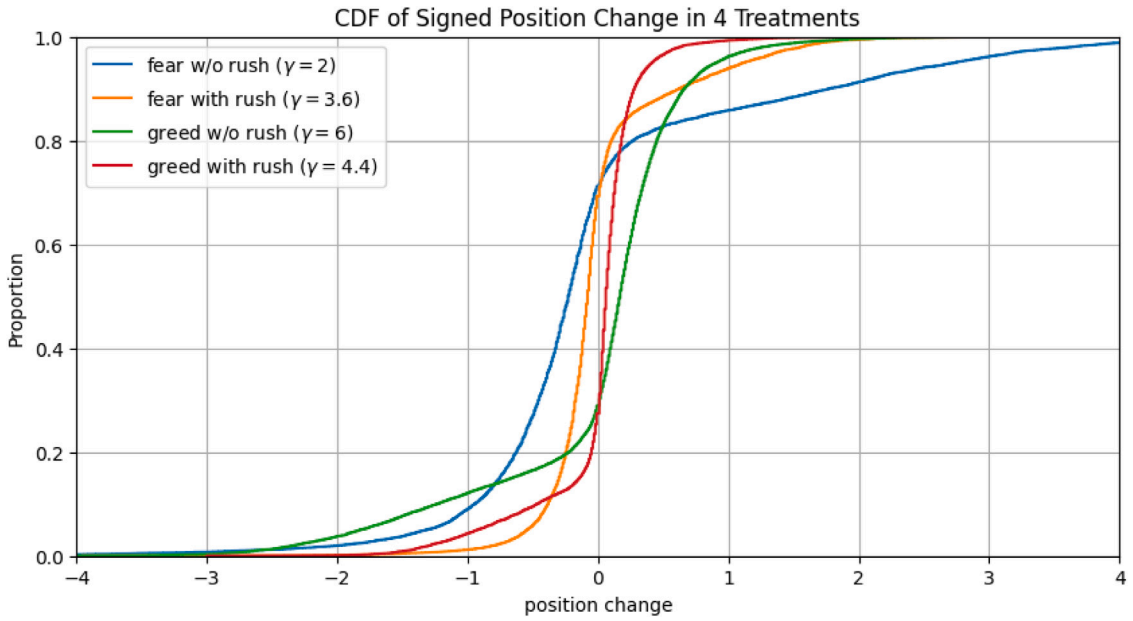

Fig. 14. Empirical cumulative distribution functions of observed moves Δx by γ treatment.

Table 7
Test of Hypothesis 4. $\#N$ and $\#P$ are counts of upward and downward moves, and the μ's are the mean absolute values of such moves. The null hypothesis for the binomial test is that upward and downward moves are equally likely. The null hypothesis for the Wilcoxon Signed Rank test is that (absolute values of) upward and downward moves have the same distributions. The notation $<^{***}$ indicates rejection (in the indicated direction) of the null hypothesis at $p < 0.01$. All observations are treated as independent.

	# N	# P	Binomial test	$\mu_N(\lvert\Delta x\rvert)$	$\mu_P(\lvert\Delta x\rvert)$	Wilcoxon signed rank test
fear without rush ($\gamma = 2$)	8576	3470	$>^{***}$	0.543	1.364	$<^{***}$
fear with rush ($\gamma = 3.6$)	7603	3370	$>^{***}$	0.222	0.506	$<^{***}$
greed without rush ($\gamma = 6$)	3902	9590	$<^{***}$	0.927	0.359	$>^{***}$
greed with rush ($\gamma = 4.4$)	3181	8419	$<^{***}$	0.431	0.167	$>^{***}$

The simulated cycles have a distinctive asymmetric pattern: most of the time they move gradually away from the harvest time $\hat{x}$ but at some point they jump most of the way back. Hypothesis 4 quantifies this pattern. It predicts that, with fear parameters, the number $\#N$ of movements $\Delta x < 0$ away from $\hat{x}$ exceeds the number $\#P$ of movements $\Delta x > 0$ towards $\hat{x}$, but the movements towards $\hat{x}$ are more sizeable ($|\Delta x|$ larger on average). With greed parameters, the roles of $\#N$ and $\#P$ are reversed.

Fig. 14 supports that prediction. For both greed cases (red and green curves), we see that the empirical cdf's cross the $\Delta x = 0$ line at about 0.3, indicating that $\#N$ represents only about 30% of observations versus about 70% for $\#P$. The orange and blue curves indicate that, as predicted, the proportions are reversed for the fear cases. Also as predicted, the upper (resp. lower) tails of the distributions are much fatter for the fear (resp. greed) parameters. For example, looking at where the curves cross $\Delta x = 1$, we see that well over 10% of location changes are positive jumps of at least 1.0 for $\gamma = 2$, representing over a third of all positive changes. In the greed cases ($\gamma = 4.4$ and 6), in sharp contrast, well under 5% of location changes are jumps of at least $\Delta x = 1$, representing less than a fifteenth of positive changes.

Table 7 reports standard tests confirming highly significant predicted asymmetries.

Result 4. *Hypothesis 4 is confirmed. Most individual location changes are short moves away from the harvest time $\hat{x}$, while moves towards $\hat{x}$ tend to be longer jumps.*

Hypothesis 5 comes from the observation that, in our dynamic simulations, the parameters we chose for safe Nash rushes tend to produce longer cycles (more time steps) than do the parameters for no Nash rushes. Table 8 investigates by pairing treatments with the same latency and fear/greed status. Using a standard bootstrap test, it confirms that in each pair there are more cycles per period in the no-rush treatment.

Result 5. *Hypothesis 5 is confirmed. Cycles are more frequent (and thus have shorter lengths) in fear treatments than in corresponding greed treatments.*

Our last hypothesis concerns payoffs, which consistently exceed the safe Nash level in our adaptive dynamic simulations. The second column of Table 4 shows that the mean ratios of empirical to safe Nash profits exceed 1.0 in all treatments. The profit ratio

Table 8
Tests of Hypothesis 5. The first four columns report the mean number of cycles (session-clustered standard errors in parentheses). Bootstrap results are based on 10,000 samples drawn with replacement from the observed sessions. The last column shows a two-sample Student t test for equality of means in bootstrap data; the notation $>^{***}$ indicates that the test rejects the null of equality in favor of the without rush ($\gamma = 2$ or 6) mean being larger with p-value < 0.01.

	Observed results		Bootstrap results		
	without rush	with rush	without rush	with rush	Two sample t-test
Latency 0.5 s					
fear ($\gamma = 2$ vs. 3.6)	10.250	8.375	10.249	8.377	$>^{***}$
	(0.500)	(1.875)	(0.354)	(1.325)	
greed ($\gamma = 6$ vs. 4.4)	10.500	9.625	10.499	9.627	$>^{***}$
	(0.250)	(1.875)	(0.177)	(1.325)	
Latency 1 s					
fear ($\gamma = 2$ vs. 3.6)	8.750	7.250	8.754	7.249	$>^{***}$
	(1.750)	(0.500)	(1.238)	(0.353)	
greed ($\gamma = 6$ vs. 4.4)	7.250	6.500	7.248	6.500	$>^{***}$
	(0.750)	(0.250)	(0.531)	(0.177)	

Table 9
Test of Hypothesis 6. Entries are mean ratio of actual payoffs to safe NE payoffs (standard errors clustered by session shown in parentheses). The notation *** indicates that the one sample t-test rejects the null hypothesis that the mean ratio is 1.0 at $p < 0.01$.

	Fear without rush ($\gamma = 2$)	Fear with rush ($\gamma = 3.6$)	Greed without rush ($\gamma = 6$)	Greed with rush ($\gamma = 4.4$)
Payoff Ratio	1.062^{***}	1.013^{***}	1.010^{***}	1.011^{***}
	(0.014)	(0.002)	(0.002)	(0.001)

is especially high for $\gamma = 2$ empirically as well as in simulations, and the empirical means are generally within a standard deviation or so of the simulation ratios (cf Table 3). Table 9 confirms, with a simple t-test with p-values < 0.01, that the payoff ratios exceed 1.0 for each γ treatment.

Result 6. *Hypothesis 6 is supported. Observed payoffs exceed safe Nash levels by proportions similar to those obtained in simulations.*

6. Conclusion

Our results can be summarized briefly. Groups of 10–12 human subjects play a set of location games in a laboratory environment that allows them to freely adjust their location in each round of play. These location games have distinctive Nash equilibrium distributions,[8] some involving many players choosing the same location ("rushes") and some involving war-of-attrition incentives ("greed") or pre-emption incentives ("fear").

Our human players' location choices are very poorly approximated by the Nash equilibrium or indeed by any fixed distribution. Instead, the location distribution usually clusters and enters a cycle. With greed incentives, most location adjustments are small and upward, ending with a large downward jump at the end of each cycle. The reverse cycle direction occurs with fear incentives. Populations of simulated adaptive agents ("bots") cycle in a similar fashion, and provide useful predictions of how the cycle frequency and domain depend on game parameters.

These results suggest several directions for new research. First, our small scale experiment was only able to investigate four different configurations of payoff parameters in each of four sessions lasting 16 rounds. We are confident that similar cycles would occur for a broad range of different parameters and nuisance variables (such as latency, number of players, and screen display) but that remains to be confirmed. For example, would it make a qualitative difference if future experiments updated the landscape display more or less often, or averaged it over time, or otherwise made it more or less informative about current payoff opportunities?

Second, we did not examine parameters (e.g., $\rho = 3, \gamma = 4$) that support multiple safe Nash equilibria. Do such parameters produce especially slow cycles that depend sensitively on initial conditions, as suggested by simulations, or just erratic behavior? Also, does Result 5 really reflect an asymmetry between fear and greed parameters or does it instead, as we suspect, reflect something about proximity to parameters that support multiple equilibria?

We hope that our experiment spurs new theoretical work. We considered only a three parameter family of rank-dependent location games. How broad is the class of location games for which we should expect cycles rather than convergence to a static Nash equilibrium? For such games, how does the cycle frequency and amplitude depend on the payoff function and the adjustment opportunities and information available to players? We have shown ways for simulations to address such questions, but more

[8] Our Nash equilibrium benchmark is for the continuum player game, due to its tractability. The finite player game has no closed form NE, but it tends to the continuum one, as the number of players grows.

definitive answers seem to require theoretical advances. In particular, our simulations use discrete time and location grids, and finite numbers of players. It would be helpful to better understand convergence to the continuum limit in time, location space and player populations.

Finally, we note that our work potentially has major repercussions for applied work. Applied researchers routinely focus their data analysis on equilibrium, especially when it is unique. Our findings suggest that focus may be misplaced, and not just for the practically important timing games in ASP, but also for pricing or quantity or attribute location games. Researchers should take seriously the possibility that some sort of cyclic process is generating the data observed in such games.

Declaration of competing interest

The authors declare that they have no known competing financial interests or personal relationships that could have appeared to influence the work reported in this paper.

Appendix A. Safe Nash equilibria of the continuum player game

A.1. Greed and fear rush sizes

We solve for the rush sizes, by equating rush payoff to marginal payoff in gradual play.

First, *not greed*. Assume $\gamma < \rho + 4/3$. The pre-emption equilibrium has an initial rush prior to the harvest time of size:

$$q_0 = \arg\max_q q^{-1} \int_0^q v(p)dp = \arg\max_q q^{-1} \int_0^q (1 - z/\gamma)(1 + z/\rho)dz \tag{3}$$

The FOC is average equals margin:

$$q + (1/\rho - 1/\gamma)q^2/2 - q^3/(3\rho\gamma) = q(1 - q/\gamma)(1 + q/\rho)$$

$$\Leftrightarrow q_0 = 3(\gamma - \rho)/4. \tag{4}$$

That is, if an partial pre-emptive fear rush exists then $q_0 = 3(\gamma - \rho)/4$. A partial fear rush exists if $\rho < \gamma < \rho + 4/3$, since $\gamma = \rho$ implies $q_0 = 0$, and $\gamma = \rho + 4/3$ implies $q_0 = 1$. The rush size q_0 grows as greed γ increases.

Next, *not fear*. Assume $\rho + 2/3 < \gamma < 2$. In the war of attrition equilibrium, the *terminal rush* has size:

$$q_1 = \arg\max_q (1 - q)^{-1} \int_q^1 v(x)dx = \arg\max_q (1 - q)^{-1} \int_q^1 (1 - z/\gamma)(1 + z/\rho)dz \tag{5}$$

The FOC, average equals margin, is now:

$$1 + \frac{1/\rho - 1/\gamma}{2} - \frac{1}{3\rho\gamma} - q - (1/\rho - 1/\gamma)q^2/2 + q^3/(3\rho\gamma) = (1 - q)(1 - q/\gamma)(1 + q/\rho)$$

As we can assume $q < 1$, we factor out $(1 - q)$. Recalling $3(\gamma - \rho) > 2$:

$$1 + \frac{1/\rho - 1/\gamma}{2}(1 + q) - \frac{1}{3\rho\gamma}(1 + q + q^2) = (1 - q/\gamma)(1 + q/\rho)$$

$$\Leftrightarrow q_1 = (3(\gamma - \rho) - 2)/4 \tag{6}$$

if an incomplete greed rush exists then $q_1 = (3(\gamma - \rho) - 2)/4$. In other words, a partial greed rush exists if $\rho + 2/3 < \gamma < \rho + 2$, since $\gamma = \rho + 2/3$ implies $q_1 = 0$ and $\gamma = \rho + 4/3$ implies $q_1 = 1$. The rush size $1 - q_1$ shrinks as greed γ increases.

A.2. Fear CDF and rush time

Using ASP's terminology, assume not greed: The pre-emption game gradual play ends at the harvest time $x^* = \lambda$. The quantile $Q_P(x)$ stopping in gradual play solves $v(Q_P(x))u(x) = v(1)u(x^*)$, and thus

$$(1 - Q_P(x)/\gamma)(1 + Q_P(x)/\rho)[1 + 2\lambda x - x^2] = (1 + 1/\rho)(1 - 1/\gamma)(1 + \lambda^2) \tag{7}$$

In other words, *the common Nash payoff is* $(1 + 1/\rho)(1 - 1/\gamma)(1 + \lambda^2)$ for all stopping times. So solving this quadratic equation, now with $c = (1 + 1/\rho)(1 - 1/\gamma)(1 + \lambda^2)/(1 + 2\lambda x - x^2)$, yields

$$\Rightarrow 2Q_P(x) = \gamma - \rho + \sqrt{(\gamma + \rho)^2 - 4\frac{(1 + \rho)(\gamma - 1)(1 + \lambda^2)}{1 + 2\lambda x - x^2}} \tag{8}$$

Equate the quantile at the start of the gradual (8) with the initial rush $Q_P(\underline{x}) = q_0$ in (4):

$$\gamma - \rho + \sqrt{(\gamma + \rho)^2 - 4\frac{(1 + \rho)(\gamma - 1)(1 + \lambda^2)}{1 + 2\lambda\underline{x} - \underline{x}^2}} = 2 \times 3(\gamma - \rho)/4$$

$$\Leftrightarrow \underline{x} = \lambda - \sqrt{1+\lambda^2}\sqrt{1 - \frac{16(1+\rho)(\gamma-1)}{(\gamma+3\rho)(3\gamma+\rho)}} \tag{9}$$

This is positive and real provided, respectively:

$$\frac{\lambda^2}{1+\lambda^2} > 1 - \frac{16(1+\rho)(\gamma-1)}{(\gamma+3\rho)(3\gamma+\rho)} > 0 \Leftrightarrow 1+\lambda^2 > \frac{(\gamma+3\rho)(3\gamma+\rho)}{16(1+\rho)(\gamma-1)} > 1 \tag{10}$$

The first inequality in (10) is required for a sufficient fundamental growth and the second holds provided

$$(\gamma+3\rho)(3\gamma+\rho) > 16(1+\rho)(\gamma-1) \Leftrightarrow [3(\gamma-\rho)-4][\gamma-\rho-4] > 0$$

With not greed, $\rho < \gamma < \rho + 4/3$, and thus $3(\gamma-\rho)-4 < 0$ and more readily $\gamma-\rho-4 < 0$.

The last inequality in (10) requires $\gamma > 1$.

A.3. Greed CDF and rush time

Next, assume *not fear*: Since the war of attrition starts with gradual play at the harvest time $x^* = \lambda$, the quantile $Q_W(x)$ stopping solves $v(Q_W(x))\pi(x) = v(0)\pi(x^*)$ and thus:

$$(1 - Q_W(x)/\gamma)(1 + Q_W(x)/\rho)(1 + 2\lambda x - x^2) = 1 + \lambda^2 \tag{11}$$

So *the Nash payoff is* $v(0)\pi(\lambda) = 1 + \lambda^2$. Put $c(x) = (1+\lambda^2)/(1+2\lambda x - x^2)$. Solving this quadratic $(1 - q/\gamma)(1 + q/\rho) = c(x)$, or $q^2 + (\rho-\gamma)q + (c(x)-1)\gamma\rho = 0$, yields:

$$Q_W(x) = \frac{\gamma - \rho - \sqrt{(\gamma-\rho)^2 - 4\rho\gamma(c(x)-1)}}{2} = \frac{\gamma - \rho - \sqrt{(\gamma+\rho)^2 - 4\rho\gamma c(x)}}{2} \tag{12}$$

Since $1 + 2\lambda x - x^2 = 1 + \lambda^2 - (\lambda - x)^2$, we have $c > 1$, and thus $q_1 > 0$. Then (11) implies

$$2Q_W(x) = \gamma - \rho - \sqrt{(\gamma+\rho)^2 - 4\rho\gamma\frac{1+\lambda^2}{1+2\lambda x - x^2}} \tag{13}$$

No one enters before the peak $x^* = \lambda$ of the hump: $Q_W(\lambda) = [(\gamma-\rho)-(\gamma-\rho)]/2 = 0$. Since $(1+2\lambda x - x^2)' = 2(\lambda - x) < 0$ for all $x > x^*$, we have $Q'_W(x) > 0$, with $Q'_W(x^*) = 0$.

Let us equate (twice) the flow rush size (6) with the terminal rush, using (13):

$$\gamma - \rho - \sqrt{(\gamma+\rho)^2 - 4\rho\gamma\frac{1+\lambda^2}{1+2\lambda\bar{x} - \bar{x}^2}} = (3(\gamma-\rho)-2)/2$$

$$\Leftrightarrow 1 + (\rho-\gamma)/2 = \sqrt{(\gamma+\rho)^2 - 4\rho\gamma\frac{1+\lambda^2}{1+2\lambda\bar{x} - \bar{x}^2}}$$

The left side is negative for $\gamma > \rho + 2$, and so no solution exists. Squaring:

$$\Leftrightarrow (\rho-\gamma)^2 + 4(\rho-\gamma) + 4 = 4(\gamma-\rho)^2 - 16\rho\gamma\frac{\lambda^2 - 2\lambda\bar{x} + \bar{x}^2}{1+2\lambda\bar{x} - \bar{x}^2}$$

$$\Leftrightarrow \bar{x} = \lambda + \frac{\sqrt{1+\lambda^2}}{\sqrt{1 + \frac{16\rho\gamma}{[3(\gamma-\rho)-2][(\gamma-\rho)+2]}}} \tag{14}$$

Since $\rho + 2/3 < \gamma < 2$, we have $2 < 3(\gamma-\rho) < 3(2-\rho)$ and so of course $\gamma - \rho > 0$, and thus $\bar{x} < \lambda + \sqrt{1+\lambda^2} \equiv x_{max}$.

Appendix B. Supplementary data

Supplementary material related to this article can be found online at https://doi.org/10.1016/j.jebo.2026.107609, which includes Appendix B: participant instructions. Other materials are posted at osf.io/rmzvb.

Data availability

Data will be made available on request.

References

Anderson, Axel, Smith, Lones, Park, Andreas, 2017. Rushes in large timing games. Econometrica 85 (3), 871–913.
Burdett, Kenneth, Judd, Kenneth L., 1983. Equilibrium price dispersion. Econ.: J. Econ. Soc. 955–969.
Cason, Timothy, Friedman, Daniel, Hopkins, Ed, 2014. Cycles and Instability in a Rock–Paper–Scissors population game: A continuous time experiment. Rev. Econ. Stud. 81 (1), 112–136.
Cason, Timothy N., Friedman, Daniel, Hopkins, Ed, 2021. An experimental investigation of price dispersion and cycles. J. Political Econ. 129 (3), 789–841.
Cason, Timothy N., Friedman, Daniel, Wagener, Florian, 2005. The dynamics of price dispersion, or edgeworth variations. J. Econom. Dynam. Control 29 (4), 801–822.
Chen, Daniel L., Schonger, Martin, Wickens, Chris, 2016. oTree—An open-source platform for laboratory, online, and field experiments. J. Behav. Exp. Financ. 9 (C), 88–97.
Edgeworth, Francis Ysidro, 1925. The pure theory of monopoly. In: Papers Relating To Political Economy, Vol. 1., Macmillan, London, pp. 111–142.
Geanakoplos, John, 2009. The leverage cycle. NBER Macroecon. Annu. 24 (1), 1–66.
Greiner, Ben, 2004. The Online Recruitment System ORSEE 2.0 - A Guide for the Organization of Experiments in Economics. Working Paper Series in Economics 10, University of Cologne, Department of Economics.
Morris, Stephen, Shin, Hyun Song, 2002. Social value of public information. Am. Econ. Rev. 92 (5), 1521–1534.
Noel, Michael D., 2007. Edgeworth price cycles, cost-based pricing, and sticky pricing in retail gasoline markets. Rev. Econ. Stat. 89 (2), 324–334.
Roth, Alvin E., Xing, Xiaolin, 1994. Jumping the gun: Imperfections and institutions related to the timing of market transactions. Am. Econ. Rev. 84, 992–1044.
Smith, Vernon L., 1962. An experimental study of competitive market behavior. J. Political Econ. 70 (2), 111–137.
Veblen, Thorstein, 1899. Mr. cummings' strictures on 'the theory of the leisure class'. J. Political Econ. 8 (1), 106–117.